On the dispersive modeling of the 2011 Tohoku tsunami generation by coseismic/SMF processes, and near- and far-field impact

Stephan Grilli[1], Jeffrey C. Harris[1,2], James T. Kirby[3], Fengyan Shi[3], Gangfeng Ma[4], Tim Masterlark[5], David Tappin[6] and Tayebeh S. Tajalli Bakhsh[1]

1. Ocean Engng. Dpt., Univ. of Rhode Island, Narragansett, RI 02882, USA (grilli@oce.uri.edu)
2. Laboratoire St Venant, EDF Chatou, France
3. Univ. of Delaware, Center for Applied Coastal Res., Newark, DE 19716, USA
4. Dept. of Civil and Environmental Engineering, Old Dominion University, Norfolk, VA 23529, USA
5. British Geological Survey, Kingsley Dunham Centre, Keyworth, Nottingham, NG12 5GG, UK
6. Department of Geological Sciences, University of Alabama, Tuscaloosa, Alabama, USA

1 Introduction

A careful modeling of the 2011 Tohoku-oki tsunami generation and coastal impact [2,3], using the latest generation dispersive/non-hydrostatic models [6,7,10] shows that its devastating coastal impact cannot be fully explained by a co-seismic source alone, even when assimilating all available geodetic data [3,8,9]. Indeed, such tsunami simulations fail to reproduce the elevated tsunami runup heights of up to 40 m along the (Sanriku) coast of northern Honshu, and the large amplitude higher frequency dispersive waves (of 3-4 min. period) recorded at offshore buoys (both GPS and DART).

Here, we identify and parameterize an additional source of generation of the higher-frequency tsunami waves, in the form of a large rotational Submarine Mass Failure (SMF), which we source north of the main rupture, based on travel time of the higher frequency waves. Using the three-dimensional (3D) (sigma-layer) non-hydrostatic model NHWAVE [7], we simulate tsunami generation triggered by a time and space dependent seafloor motion, due to the combination of: (i) a new co-seismic source based on a detailed 3D Finite Element Modeling (FEM) of the heterogeneous subduction zone, with geodetic data assimilation, that updates our earlier source [2,3]; and (ii) the additional tsunami source from the SMF, triggered with a 2 time delay, whose kinematics is specified based on earlier scaling and modeling work [4].

After 5 min. of simulations, tsunami waves are reinterpolated onto the nonlinear and dispersive model FUNWAVE two-dimensional grid, in Cartesian coordinates for near-field simulations [10] and in spherical coordinates for far-field simulations [5]. Various levels of grid nesting are used, both in near- and far-field, with bathymetric/topographic data of commensurate accuracy. In results, briefly summarized below, we show that the multi-source tsunami simulation results agree well with all the available near-field observations, both onshore (runup/inundation) and offshore (GPS and DART buoy data), as well as far-field observations (DART buoys), as far as South America. It should be stressed that this good agreement is achieved without assimilating any of the tsunami observations in the source (which most of the models proposed to date have done). Hence, our simulations are robust.

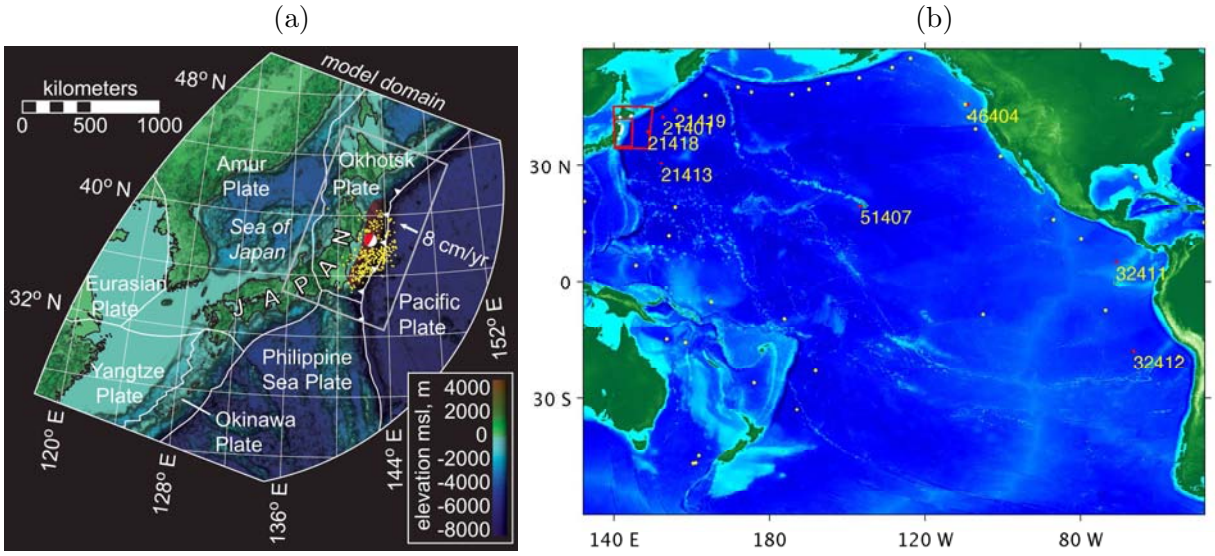

Figure 1: (a) Tohoku 2011 M9.1 earthquake seismotectonics (rupture is red polygon) and FEM domain ("model domain"); large symbol is the epicenter; yellow dots show M > 4 aftershocks (11 March – 06 May 2011); the Pacific-Okhotsk plate convergence is about 8 cm/yr. (b) Computational domains for FUNWAVE simulations: (i) near-field (regional 1000 m resolution, 800 by 1200 km, and coastal 250 m, large/small red boxes) Cartesian grid (large one also for NHWAVE); and (ii) far-field (Pacific basin scale) 2' spherical grid from 132° E to 68° W and 60° S to 60° N), with marked location of 18 DART buoys (yellow/red dots) and nearshore GPS buoys (white dots).

2 Methodology and results

Fig. 1 shows the seismotectonic context near and around the Japan trench relevant to the Tohoku-Oki tsunami as well as computational grids used in NHWAVE and FUNWAVE simulations. The co-seismic and SMF sources are first modeled for 300 s (5 min.) in a 1 km mesh regional grid, using NHWAVE, as a time- and space- varying bottom boundary condition (Fig. 1). Results are then re-interpolated into the fully nonlinear and dispersive Boussinesq model FUNWAVE for further modeling. Bathymetry/topography data bases are used, from ETOPO1 in deep water to 50 m accurate data (and model grids) nearshore and onshore. Simulations are compared to GPS and DART buoy time series (Fig. 3) and maximum runup (Fig. 4) and flow depth/inundation.

Although there are not yet any direct geological observations of the proposed SMF, its location and kinematics were identified and validated by travel-time analysis of higher-frequency waves recorded at GPS and DART buoys, and many direct SMF tsunami simulations. Additionally the proposed SMF source is justified from both the known geology of the Japan Trench, slope stability analyses, and tsunami runups and inundation limits recorded during post-tsunami field surveys [1,5]. Finally, a difference bathymetry map between post- and pre-earthquake data (not shown here for lack of space) shows large vertical seafloor deformations at the right location, consistent with our proposed SMF mechanism and kinematics.

Results in Fig. 2a show, at time t = 5min., the generation of both two long and nearly parallel leading co-seismic tsunami elevation waves to the south and a series of shorter (and hence dispersive) crescent shape SMF tsunami waves to the north. At t = 15 min., Fig. 2b shows that while the co-seismic waves do not develop a dispersive tail, the SMF waves develop into a train of

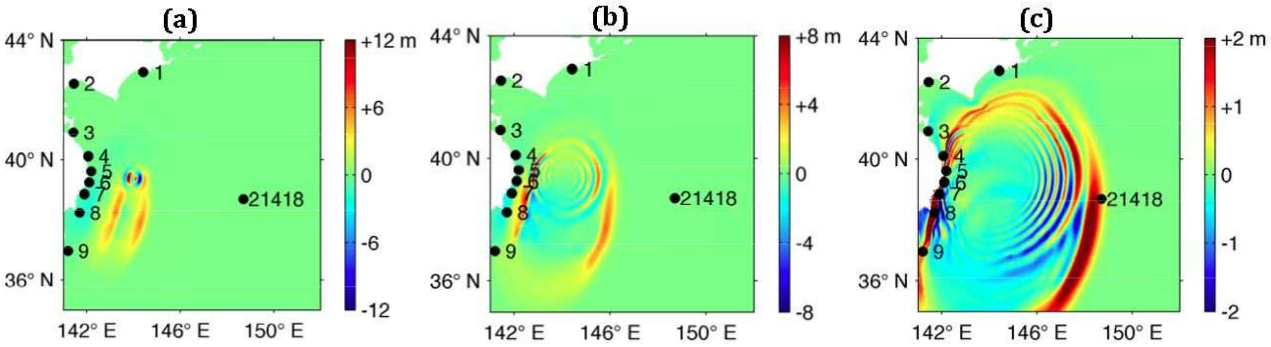

Figure 2: NHWAVE-FUNWAVE simulations using the combined co-seismic/SMF source, showing instantaneous surface elevations at t = (a) 5; (b) 15; (c) 30 min., in 1 km FUNWAVE grid (Fig. 1b). Labeled black dots mark locations of GPS buoys and of DART buoy #21418 (Fig. 3). Note the highly dispersive nature of waves generated by the SMF source triggered to the north (135 s after the co-seismic source), as compared to the longer non-dispersive co-seismic tsunami waves generated to the south.

concentric shorter waves, whose maximum elevations (both on- and offshore) are narrowly focused. Fig. 2c shows at $t = 30$ min., that the leading offshore co-seismic tsunami wave reaches the nearest DART buoy #21418, and is closely followed by at least 6 of the shorter oscillatory waves generated by the SMF. Fig. 3d shows the time series of both the simulated and observed waves at this DART buoy; their agreement is very good. Onshore, Fig. 2c shows that the same waves impact the 3 GPS buoys (Nb. 4,5,6) off of the Sanriku coast where maximum runup was measured at or slightly before the same time. Figs. 3a-c show the time series of both the simulated and observed waves at these GPS buoys; their agreement is also very good. Fig. 3 also shows that simulations of the co-seismic tsunami without the SMF waves do not reproduce the observed shorter/dispersive waves at the GPS and DART buoys.

Having been able to accurately match observations at the various buoys, with results of the simulations for the combined co-seismic/SMF tsunami source, we now compare in Fig. 4 simulated runups and inundations along the coast of northern Honshu. We see that simulations with the combined co-seismic/SMF tsunami source accurately simulate observed runups and inundations, including the 40+ m values along the Sanriku coast. By contrast, simulations with only the co-seimsic source underpredict the latter by a factor of 3. Additional results showing a comparison of far-field simulations with observations at DART buoys as well as a discussion of dispersive and Coriolis effects in the far-field tsunami will be presented during the workshop.

3 References

1. Fujiwara, T., Kodaira S., No T., Kaiho Y., Takahashi N. and Kaneda Y. (2011). Tohoku-Oki earthquake: Displacement reaching the trench axis. *Science*, **334**(6060):1240.

2. Grilli, S.T., Harris J.C., Tajali Bakhsh T.S., Kirby J.T., Shi F., Masterlark T.L. and Kyriakopoulos C. (2012a). Numerical simulation of the 2011 Tohoku tsunami: Comparison with field observations and sensitivity to model parameters. *Proc. 22nd Offshore and Polar Engng. Conf.* (Rodos, Greece, 6/17-22/2012), 6-13.

3. Grilli, S.T., Harris, J.C., Tajali Bakhsh, T.S., Masterlark, T.L., Kyriakopoulos, C., Kirby, J.T. and and Shi, F. (2012b). Numerical simulation of the 2011 Tohoku tsunami based on a new transient FEM co-seismic

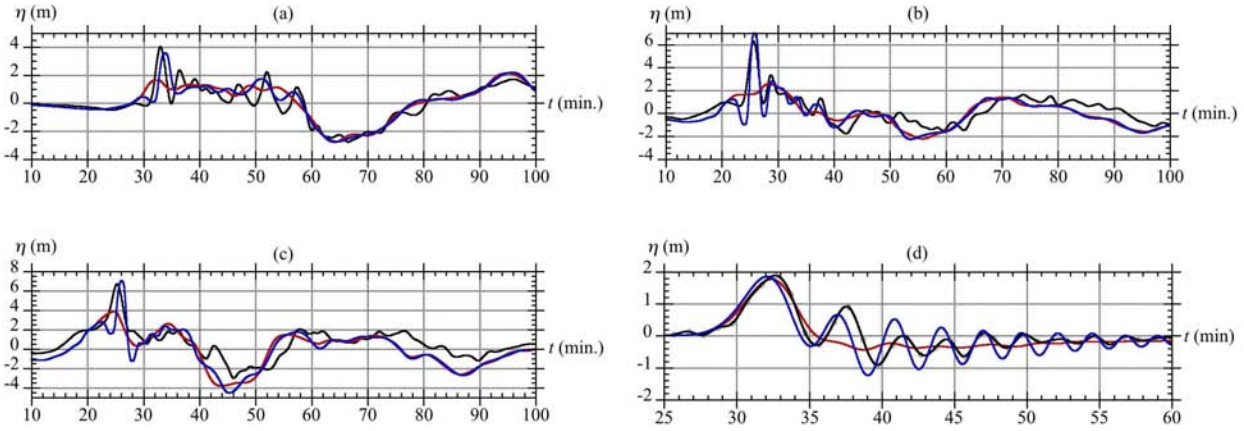

Figure 3: Surface elevations at buoys near Japan as a function of time, for 4th-6th GPS stations (marked in Figs. 1,2): (a) North Iwate; (b) Central Iwate; (c) South Iwate; and (d) DART buoy #21418. Field measurements (black), and computations for the co-seismic source alone (red), and for the latter plus the SMF source (blue). The abscissa is time t in minutes from the start of the earthquake rupture.

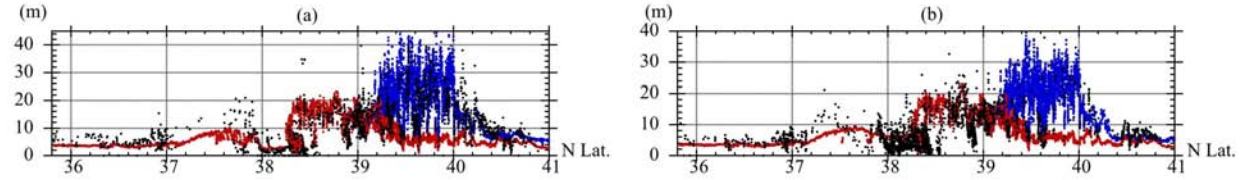

Figure 4: Comparison of simulated runup (a) and inundation (b) with measurements (black dots), for: co-seismic source alone (red), and combined co-seimsic/SMF source (blue).

source: Comparison to far- and near-field observations. *Pure and Appl. Geophys.*, DOI 10.1007/s00024-012-0528-y (published online).

4. Grilli, S.T. and P. Watts. 2005. Tsunami generation by submarine mass failure Part I : Modeling, experimental validation, and sensitivity analysis. *J. Waterw. Port Coast. and Oc. Engng.*, **131**(6), 283-297.

5. Kawamura, K., Sasaki, T., Kanamatsu, T., Sakaguchi, A., Ogawa Y. (2012). Large submarine landslides in the Japan Trench: A new scenario for additional tsunami generation. *Geophys. Res. Lett.*, **39**:L05308.

6. Kirby J.T., Shi F., Harris J.C., and Grilli S.T. (2012). Dispersive tsunami waves in the ocean: Model equations and sensitivity to dispersion and Coriolis effects. *Ocean Modell.* (in press):18 pp. http://dx.doi.org/10.1016/j.ocemod.2012.11.009.

7. Ma G., Shi F. and Kirby J.T. (2012) Shock-capturing non-hydrostatic model for fully dispersive surface wave processes. *Ocean Modell.*, **43-44**:2235.

8. Masterlark, T. (2003). Finite element model predictions of static deformation from dislocation sources in a subduction zone: Sensitivities to homogeneous, isotropic, Poisson-solid, and half-space assumptions. *J. Geophys. Res.*, **108**(B11):296.

9. Masterlark, T., and Hughes K. (2008). The next generation of deformation models for the 2004 M9 Sumatra-Andaman Earthquake. *Geophys. Res. Lett.*, **35**:L035198.

10. Shi, F., Kirby, J.T., Harris, J.C., Geiman, J.D. and Grilli, S.T. (2012) A high-order adaptive time-stepping TVD solver for Boussinesq modeling of breaking waves and coastal inundation. *Ocean Modell.*, **43-44**:3651.